Radiology of the hand

Marc Williams

David Temperley

Raj Murali

Abstract

This is an overview of radiological imaging of the hand highlighting the various imaging modalities used in the work-up and diagnosis of a range of orthopaedic and rheumatological disorders. The biomechanics and anatomy of the human hand is extremely complex, and a good understanding is required to diagnose pathology. In this article we explain the anatomy and highlight pathology of the hand from a radiological perspective with respect to plain film, CT, ultrasound and MR imaging. Trauma of the hand is extremely common and radiology plays an important role in the diagnosis of treatable injuries including fractures, dislocations and ligament tears. Plain radiography and CT are excellent at evaluating bony injury (e.g. Rolondo or Bennett's fracture) whereas ultrasound and MR are better at evaluating soft tissue injury (e.g. Stener lesion). The hands are a common location for degenerate and inflammatory arthropathies which all have hallmark radiological features. Radiology also plays an important role in the diagnosis and work-up of bone lesions in the hand including enchondromas, osteoid osteomas and chondrosarcomas.

Keywords arthritis; bone lesions; hand; imaging; radiology; trauma

Introduction

The human hand is a very complex structure that allows us to perform fine motor skills that are essential to our everyday living. There are a number of conditions that can affect the hand that can lead to significant dysfunction and disability. This article describes the normal radiological anatomy of the hand and the use of various imaging modalities in the diagnosis of a range of hand pathologies.

Anatomy

In humans, each hand is composed of 19 bones (five metacarpals and fourteen phalanges). Each finger contains three phalanges (proximal, middle and distal) except for the thumb, which has two phalanges (proximal and distal). In addition, most people have five sesamoid bones in each hand, two at the thumb metacarpophalangeal joint (MCPJ), one at the thumb interphalangeal joint (IPJ), and one each at index and little finger MCPJs.[1]

***Marc Williams** FRCR MBChB BSc Radiology Fellow, Robert Jones and Agnes Hunt Orthopaedic Hospital NHS Trust, Oswestry, UK. Conflicts of interest: None declared.*

***David Temperley** MBBCh BAO MRCPI FRCR BA Consultant Radiologist, Wrightington, Wigan and Leigh NHS Foundation Trust, Wigan, UK. Conflicts of interest: None declared.*

***Raj Murali** MBBS FRCSEd FRCS (Tr & Orth) Consultant Orthopaedic Surgeon, Wrightington, Wigan and Leigh NHS Foundation Trust, Wigan, UK. Conflicts of interest: None declared.*

There are multiple small joints in the hands including connection between the carpal bones of the wrist and the proximal ends of the metacarpals called the carpometacarpal joints (CMCJs). Between the metacarpals and proximal phalanges are the MCPJs, and further distally are the proximal interphalangeal joint (PIPJ) and distal interphalangeal joint (DIPJ). The thumb with two phalanges has a single IPJ (Figure 1).

The plain radiograph is an extremely important radiological examination and often the primary investigation performed in the diagnosis of traumatic bone injury and joint pathology.

There are multiple muscles and tendons in the hand. These can be divided into two main groups; intrinsic and extrinsic muscles. Intrinsic muscles arise from within the hand itself, whereas extrinsic muscles originate in the forearm and insert onto the bones of the hand via long tendons crossing the wrist joint. These tendons are the volar flexors and dorsal extensors.

The volar flexor tendons for each digit are composed of both flexor digitorum profundus (FDP) and flexor digitorum superficialis (FDS) which run parallel together with FDS lying superficial to the FDP tendon. The FDP tendon inserts onto the distal phalanx. The FDS tendon splits at the level of the MCP joint, with each limb passing to the sides of the FDP tendon before inserting onto the basal sides of the middle phalanx. High-frequency ultrasound can be used to evaluate the relationship and insertion of these tendons as demonstrated in Figure 2.

Each flexor tendon passes through a fibrosseous tunnel that consists of five annular pulleys (A1-A5) and three cruciform pulleys (C1-C3). They secure the tendon from proximal to distal to the adjacent phalanges to prevent bowstringing on flexion and facilitate smooth gliding of the tendons. If the tendon or pulley becomes thickened this can cause bunching and locking of the tendon known as trigger finger which can be assessed with ultrasound.

The dorsal extensors of the digits consist of extensor digitorum communis, extensor indicis proprius, and extensor digiti minimi. The extensor digitorum tendon for each digit has a central slip that inserts onto the base of the middle phalanx and two lateral bands that pass on either side of the central slip and attach to the base of the distal phalanx. Ultrasound can be used to assess these tendons (Figure 2).

For the thumb flexor and extensor tendons. On the volar side is the extrinsic flexor pollicis longus tendon that passes between the two heads of the flexor pollicis brevis muscle and inserts at the distal phalanx. On the dorsal extensor aspect there are three tendons the abductor pollicis longus (APL), extensor pollicis brevis (EPB), and extensor pollicis longus (EPL). The APL and EPB tendons are located within the first extensor compartment of the wrist. APL attaches to the base of the first metacarpal and EPB to the proximal phalanx. EPL lies within the third extensor compartment of the wrist crossing over distally and inserting onto the distal phalanx of the thumb.[2] These tendons can also be traced and evaluated using high frequency ultrasound and MR imaging.

Other important structures in the hand that can be assessed radiologically include the volar plate and collateral ligaments. The volar plate is a fibrocartilaginous structure located at the volar aspect of the MCPJ and IPJ, it helps to reinforce the joint capsule and limit hyperextension. Collateral ligaments are also important in stabilizing the MCPJ and IPJ. On ultrasound collateral ligaments are usually seen as thin echogenic or on MR

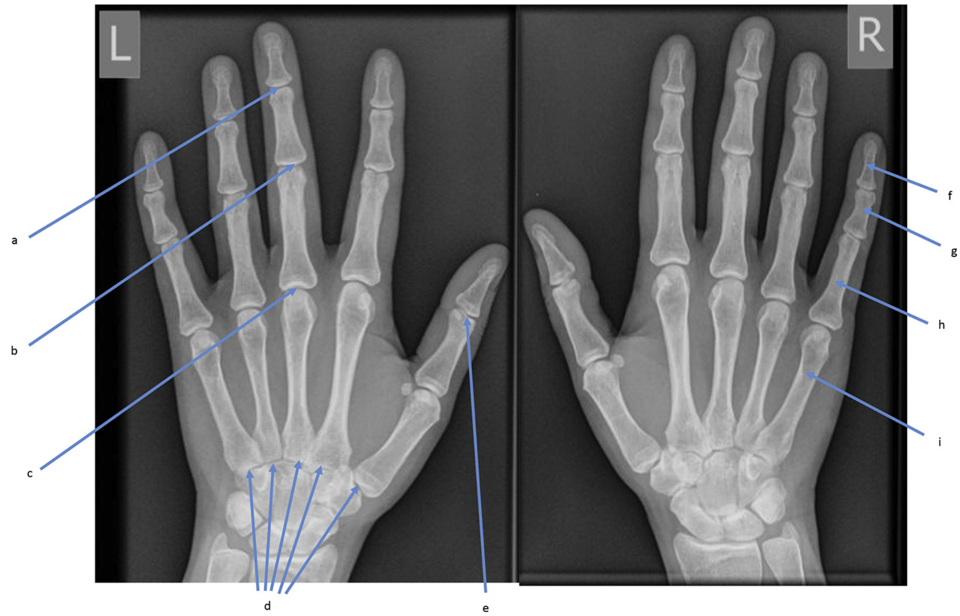

Figure 1 Normal anteroposterior radiograph of both hands. a, distal interphalangeal joint; b, proximal interphalangeal joint; c, metacarpophalangeal joint; d, carpometacarpal joints; e, interphalangeal joint; f, distal phalanx; g, middle phalanx; h, proximal phalanx; i, metacarpal.

low signal bands crossing the joint and inserting onto the adjacent bony boundaries.[3]

Trauma

Trauma of the hand is common and can lead to significant disability and loss of function if not diagnosed and treated early. Fractures of the hand account for 19% of all fractures presenting to the accident and emergency department with the little finger ray being the most commonly injured.[4]

The plain radiograph is usually the first-line investigation in the assessment of hand fractures. It can evaluate the fracture morphology (e.g. transverse, oblique or spiral); its location (i.e. neck, shaft or base); any intra-articular extension; comminution; impaction; displacement; angulation and other associated fractures or dislocations. In complex cases and for preoperative planning a CT with multiplanar bone reformats is usually performed to fully assess the fracture and its orientation.

Boxer fracture is the most common type of metacarpal fracture; it is typically a transverse fracture through the neck of the little finger metacarpal with palmar angulation of the distal fragment as shown in Figure 3. Palmar angulation is best assessed on the lateral view radiograph with lines drawn through the medullary canal.[5] It is commonly seen in young patients following a punch or impaction injury. Fractures can also be intra-articular and associated with CMC joint subluxation.

In the trauma context the base of the fourth and fifth metacarpals are important review areas particularly in a patient following a punch injury with no obvious fracture seen on the plain film. This is because overlap of the metacarpal bases with the carpal bones can be very subtle and easily missed but can

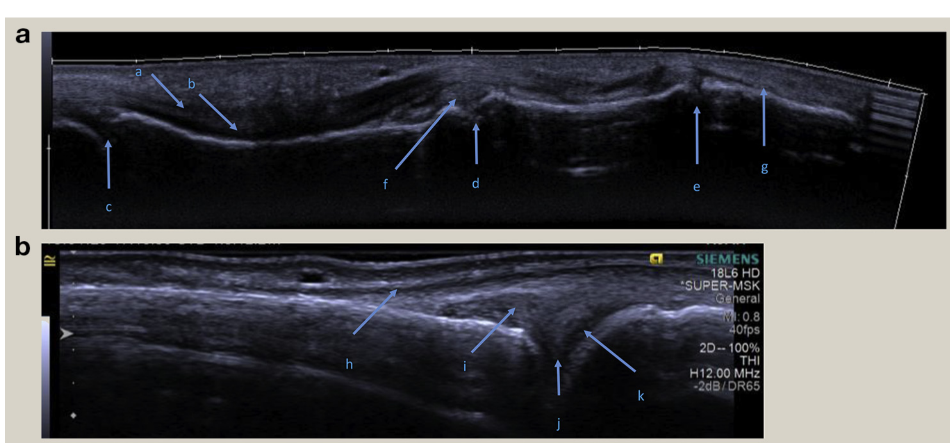

Figure 2 (a) Ultrasound extended view of the flexor digit tendons. **(b)** Ultrasound of extensor digit tendon. a, flexor digitorum superficialis; b, flexor digitorum profundus (FDP); c, metacarpophalangeal joint (MCPJ); d, proximal interphalangeal joint; e, distal interphalangeal joint; f, volar plate; g, distal insertion of FDP; h, extensor digitorum; i, triangular connective tissue; j, MCPJ; k, hyaline articular cartilage.

Figure 3 Boxer's fracture of the fifth metacarpal.

indicate significant bony trauma. Figure 4 is a case highlighting this point of a young patient following a punch injury. Plain radiograph shows no obvious fracture but there is overlap at the base of the fourth and fifth metacarpals with the hamate carpal bone. A CT scan was performed showing subluxation of the fourth and fifth CMCJs and fractures of the hamate and capitate bones. Patient went on to have surgical fixation.

There are two important eponymous fractures that involve the thumb. A Bennett's fracture is an intra-articular two-part fracture of the base of the first metacarpal bone. It is often a result of forced abduction. A Rolando fracture is similar to Bennett's but the fracture is comminuted i.e. three parts or more (Figure 5), is usually a result of an axial blow to a partially flexed metacarpal and has a poorer prognosis. Both fractures can be shown on plain radiograph but often these fractures are unstable and require surgery and so a CT is performed to aid preoperative planning. A pseudo-Bennett fracture is an extra-articular two-part fracture of the thumb metacarpal, that can be transverse or oblique. They are usually stable fractures and depending on degree of displacement and angulation are often treated conservatively.

The plain radiograph can diagnose bony volar plate avulsion injuries that occur at the proximal interphalangeal joint (PIPJ) commonly as a result of forced hyperextension. On radiograph a small avulsed fragment of bone is seen at the base of the volar aspect of the middle phalanx as demonstrated in Figure 6a. Soft tissue volar plate injuries are not detectable on plain radiograph but can be demonstrated on ultrasound and MR imaging. Figure 6b demonstrates high signal oedema in the volar plate of the little finger indicating soft tissue volar plate injury/tear**.**

Whilst the plain radiograph is excellent at demonstrating the majority of fractures in the hand, some fractures are occult or too subtle to detect. In these cases, clinicians will often request further imaging in the form of CT or MR. MR is the most sensitive imaging modality for diagnosing undisplaced or trabecular fractures by demonstrating bone marrow oedema. Fluid-sensitive fat suppressed sequences (e.g. STIR; short tau inversion recovery) are the most sensitive in the detection of bone oedema and therefore diagnosing occult fractures. T1 weighted MR images can also demonstrate low signal fracture lines. CT has an important role in diagnosing occult hand fractures and is very easily available. It can evaluate fracture configuration for preoperative planning and asses for any evidence of healing.[6]

For assessment of soft tissue injuries, high-frequency ultrasound and MR are the best imaging modalities.

Boxer knuckle is caused by the disruption of sagittal bands as a result of acute direct trauma or chronic repetitive trauma, typically seen in boxers. Sagittal bands are the main stabilizers of the extensor tendon at the MCPJ during flexion and extension. Sagittal bands exert tensile forces during flexion that prevent the

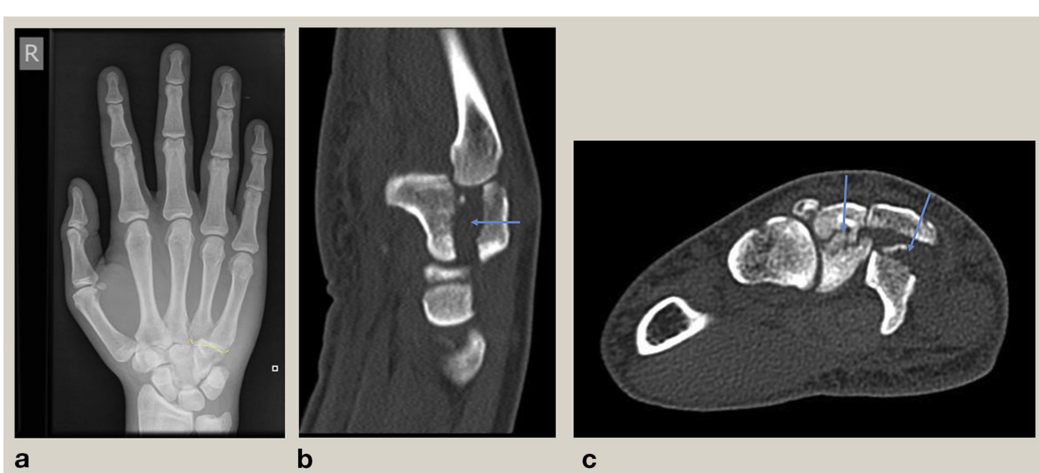

Figure 4 (a) Anteroposterior hand radiograph demonstrating overlap of the bases of the fourth and fifth metacarpals with the hamate following a punch injury. **(b)** Sagittal and **(c)** axial CT images of the hand/wrist in the same patient showing subluxation of the fifth carpometacarpal joint with associated hamate and capitate fractures.

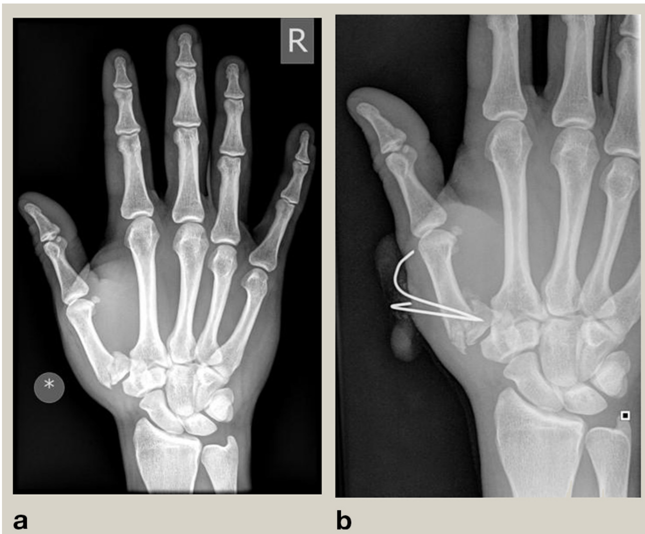

Figure 5 Rolando fracture. (**a**) Anteroposterior (AP) radiograph of the hand demonstrates a comminuted intra-articular fracture at the base of the thumb metacarpal, known as Rolando fracture. (**b**) AP radiograph of same patient showing post K-wire surgical fixation.

Figure 6 Bony and soft tissue volar plate injury. (**a**) Lateral radiograph of the index finger shows a small avulsed fragment at the volar base of the proximal phalanx in keeping with bony volar plate injury. (**b**) Sagittal MR fluid sensitive STIR image of a different patient showing high signal at the volar plate indicating oedema/soft tissue injury.

tendon from dislocating in either radial or ulnar directions. The third finger is the commonest location for this injury.[7] On ultrasound the sagittal band can appear hypoechoic and thickened and on dynamic examination the extensor tendon can be subluxed or dislocated during finger flexion.[8]

Ultrasound can be used in the assessment of pulley injuries of the digits which are prevalent amongst extreme rock climbers. On ultrasound a pulley injury will demonstrate abnormal hypoechoic thickening or non-visualization. A practical indirect sign of pulley injury is volar displacement of the flexor tendon, called bowstringing. This can be demonstrated dynamically on forced finger flexion, as the finger is flexed the distance between the flexor tendon and the underlying bone increases. The A2 pulley is the most commonly injured pulley.[9]

Trigger finger is another condition in the hand, involving impairment of the gliding movement of the flexor tendons caused by tendon constriction due to thickening of the A1 pulley or tendon sheath. On ultrasound, hypoechoic thickening of the A1 pulley at the level of the MCPJ and buckling of the tendon as it passes beneath the pulley on forced finger flexion can be demonstrated.[10]

Collateral ligament injuries of the digits can be evaluated radiologically. A radiograph is usually the first-line investigation as can often give the diagnosis by demonstrating an avulsion fracture, usually at the base of the proximal phalanx. It can also evaluate for any joint instability e.g. joint space widening or subluxation. For X-ray occult injuries MR or US can be used. On ultrasound an injured collateral ligament may appear hypoechoic or swollen, or there may be partial or complete discontinuity of the ligament fibres indicating a partial or full thickness tear. On MR, findings include soft tissue and bone marrow oedema, and discontinuity of ligaments which are seen as low signal linear bands, best seen in the coronal plane.

A gamekeeper's or skier's thumb, is an ulnar collateral ligament injury of the thumb caused by forced abduction. An

Figure 7 Anteroposterior radiograph of the right hand demonstrating osteoarthritis at the first carpometacarpal joint characterized by loss of joint space, subchondral scleosis and osteophyte formation.

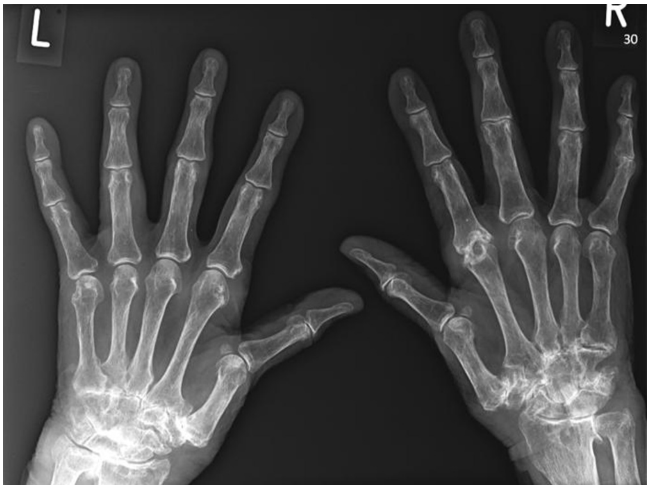

Figure 8 Anteroposterior radiograph of both hands in patient with rheumatoid arthritis. It demonstrates a proximal inflammatory arthropathy involving the wrist and metacarpophalangeal joints with osteopenia, joint space loss and bony erosions.

important finding to identify is the presence of a Stener lesion, a displaced full-thickness distal UCL tear at the first MCPJ. The UCL is displaced proximal to the MCPJ and adductor pollicis aponeurosis. Without surgery this lesion will not heal and can lead to permanent instability and dysfunction. On ultrasound a Stener lesion will appear as hypoechoic rounded structure located proximal to MCPJ. A hyperechoic focus attached to the retracted ligament casting an acoustic shadow is characteristic of a bone avulsion. On MR the appearances of a Stener lesion have been compared to a 'yo-yo on a string'. The string represents the adductor pollicis aponeurosis and yo-yo the retracted and proximally displaced UCL.[11]

Arthritis

Radiology plays a very important role in the clinical work-up of patients with suspected joint problems including inflammatory and non-inflammatory arthropathies. The bilateral hand radiograph is usually the first-line investigation as it is very easy to perform and gives an excellent overview of joint pathology in the hands.

Osteoarthritis (OA) is the most common joint disease. It is a degenerative condition and therefore tends to occur in older patients. The hallmark radiological features on plain radiograph are joint space loss, subchondral sclerosis and osteophyte formation (Figure 7). Osteoporosis and erosions can be seen in the uncommon erosive variant. OA can affect any joint in the hand but most commonly affects the distal and proximal interphalangeal joints (DIPJ, PIPJ) and the base of the thumb at the CMCJ and scaphotrapeziotrapezoidal joint (STTJ). Degenerate changes at the thumb CMCJ and STTJ are seen in approximately 30% of hand radiographs.[12] This distribution of disease is useful in differentiating OA from inflammatory arthritides.

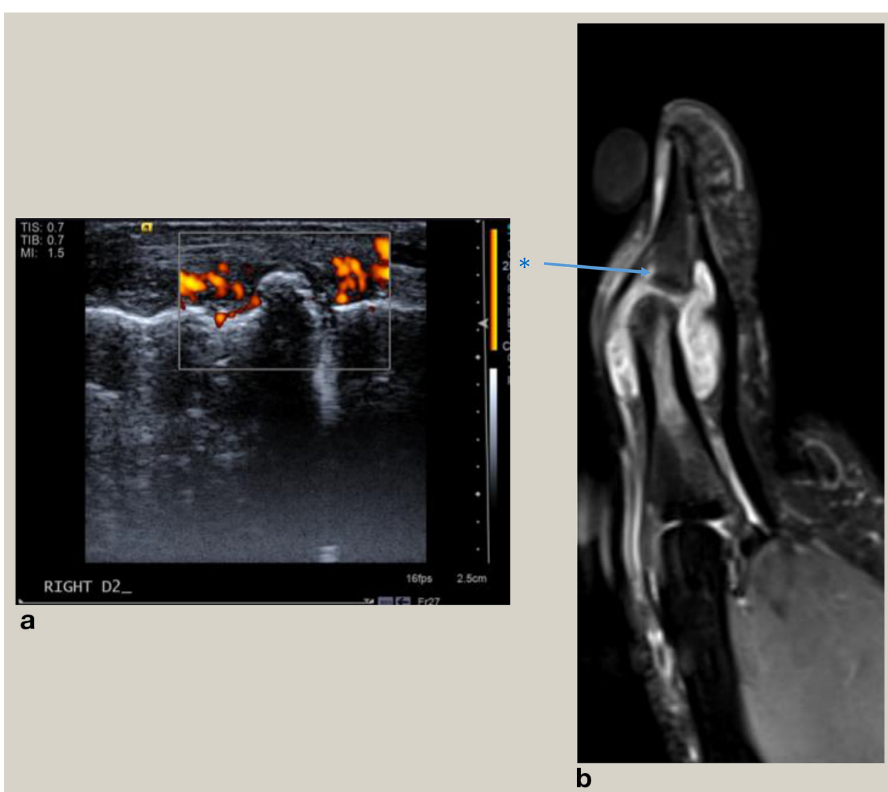

Figure 9 (**a**) Ultrasound image of second metacarpophalangeal joint demonstrating synovial thickening with increased vascularity on colour Doppler in keeping with active synovitis. (**b**) Sagittal MR fluid sensitive STIR image in a patient with inflammatory arthroapthy. It shows a large effusion at the proximal interphalangeal joint of the thumb with small erosion at the dorsal distal phalanx (*).

Figure 10 (**a**) Anteroposterior radiograph demonstrating typical appearance of an enchondroma in the middle phalanx. (**b**) Anteroposterior radiograph of both hands demonstrating multiple enchondromas in the hands in keeping with Ollier's disease.

Rheumatoid arthritis (RA) is a progressive inflammatory disorder that can affect any synovial joint in the body. The radiological hallmarks include soft tissue swelling, osteopenia, joint space loss and marginal erosions[13] (Figure 8). Erosion of the ulnar styloid is one of the earliest signs on plain radiograph and in the later stages, joint subluxation causing ulnar deviation of the MCPJs and swan neck and boutonniere deformities are seen. It can be difficult to differentiate RA from other inflammatory arthritides such psoriatic arthritis (PA) but there are certain specific characteristics one can look for. In the hands RA is classically a proximal process, affecting the MCPJ and PIPJ and sparing the DIPJ, it also tends to be bilaterally symmetric. In PA there is a distal predominance affecting the DIPJs, it is bilaterally asymmetric, and the bone density is preserved. PA is also associated with periostitis and bony ankylosis across joints.

In the early stages of inflammatory joint disease, the plain radiograph is often normal. Ultrasound is very sensitive at evaluating the soft tissues and detecting early abnormalities associated with inflammatory arthritis including joint effusions, synovial thickening, and tenosynovitis. Power Doppler can also be used to look for increased vascularity to indicate active synovitis (Figure 9a). MR is also useful at showing joint effusions, synovitis and bone erosions (Figure 9b).

The crystal-induced arthritides include gout and calcium pyrophosphate dehydrate disease (CPPD) also known as pseudogout. Gout is a metabolic disorder that results in hyperuricaemia and leads to monosodium urate crystal deposition in articular cartilage. It usually takes 4–6 years before gout is evident radiographically and so the majority of patients are treated before features develop. The hallmark radiographic features of gout

Figure 11 (a) Anteroposterior radiograph and **(b)** coronal T1 MR image of the hand demonstrating an aggressive bone lesion in the proximal and middle phalanges of the middle finger, cortical destruction, soft tissue mass with internal mineralisation. Histopathology confirmed a diagnosis of chondrosarcoma.

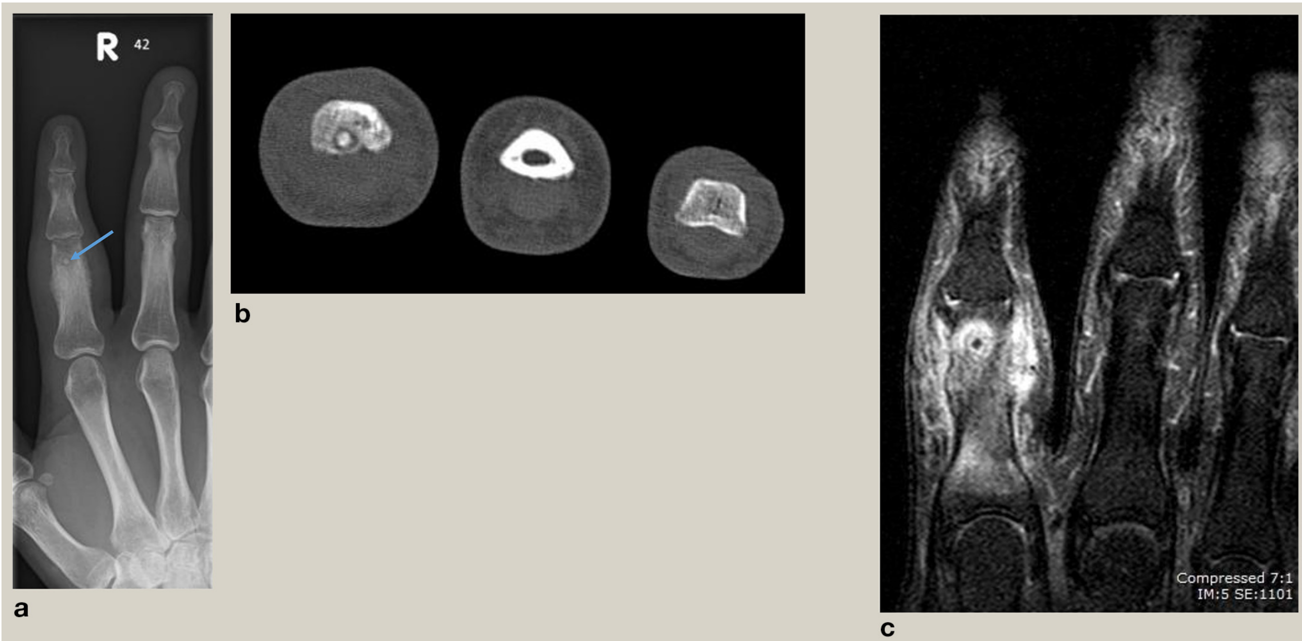

Figure 12 Osteoid osteoma (OO). **(a)** Anteroposterior radiograph of the hand demonstrates a rounded lucency with central sclerotic focus in the proximal phalanx of the ring finger with local periosteal reaction and soft tissue swelling (dactylitis). (**b**) Axial CT image showing lucent nidus with central sclerotic focus and surrounding bone formation in keeping with OO. (**c**) Coronal MR STIR sequence demonstrating marked surrounding bone marrow oedema with central sclerotic low signal focus typical of OO.

include well-defined erosions, with sclerotic margins and overhanging edges, and high-density soft tissue nodules called gouty tophi. It can affect any joint and has a random distribution in the hands. CPPD is associated with chondrocalcinosis that can be detected on plain film. The triangular fibrocartilage complex (TFCC) in the wrist is a common site and so should be carefully evaluated.

Bone and soft tissue lesions

A relatively common benign medullary bone lesion in the phalanges of the hand is a cartilage based lesion called an enchondroma. Its typical features on plain film are a well-defined, slightly expansile lucent lesion, centred in the medullary cavity with endosteal scalloping (Figure 10a), they are often incidental findings but can present with pathological fracture. Whilst most enchondromas contain calcified chondroid matrix, which can be seen on plain film but better appreciated on CT, this is not the case in the phalanges where they are often only cystic in appearance. Multiple enchondromas in the hand are seen in a condition called Ollier's disease (Figure 10b).

It can be difficult to differentiate an enchondroma from a low grade malignant chondrosarcoma. Important features to look out for are periostitis and cortical breach as these are not associated with a benign enchondroma. Also any bone oedema (without fracture) or soft tissue component on MR is concerning for malignancy.

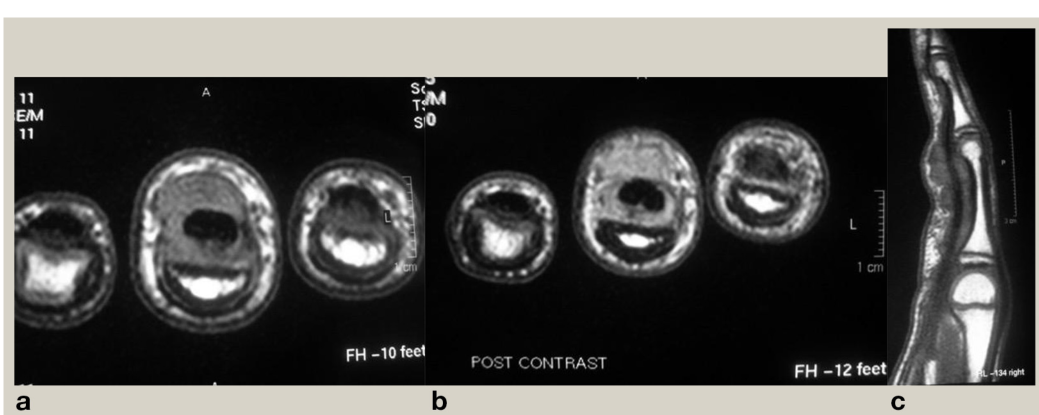

Figure 13 Tendon sheath giant cell tumour (GCT). (**a**) Axial T1 pre-contrast MR image shows a soft tissue mass encasing the flexor tendon of the ring finger which illustrates enhancement on the (**b**) post-contrast sequence. (**c**) Sagital T1 MR image demonstrates soft tissue mass at the flexor tendon at the level of the proximal interphalangeal joint. No underlying bone abnormality. Biopsy confirmed GCT of the tendon sheath.

Chondrosarcomas are malignant primary cartilaginous bone tumours that most commonly occur in patients older than 40 years of age. Although typically they occur within the long bones they can occur in the hands as a result malignant transformation from a pre-existing cartilagous tumour such as an enchondroma or osteochondroma. They are classically lytic aggressive lesions with associated soft tissue mass with internal amorphous, snowflake calcification. (Figure 11).

Osteoid osteoma is a benign bone-forming tumour that typically occurs in younger patients. Figure 12 is a case of an osteoid osteoma in the proximal phalanx of the index finger. The plain radiograph demonstrates a rounded lucency called the nidus with a central sclerotic focus. There is marked surrounding periosteal reaction and soft tissue swelling. The nidus is better visualized on the CT and typical marked surrounding bone marrow oedema is shown on the MR.

Giant cell tumours of the tendon sheath are uncommon soft tissue tumours that tend to occur in the hand and arise from the tendon sheath on the volar surface of the digits (Figure 13). Although they can cause pressure erosion of the underlying bone seen on plain film and CT they are best demonstrated on ultrasound and MR. On ultrasound the lesions are usually homogenously hypoechoic with some internal vascularity; on dynamic scanning there is free movement of the tendon within the lesion. On MR these lesions tend to be low signal on T1 and T2 sequences and demonstrate moderate contrast enhancement.[14]

Conclusion

Radiology plays an important role in the diagnosis and management of a range of pathologies in the hand. The anatomy of the hand is extremely complex and therefore knowledge of this and what the various imaging modalities can offer will help provide patients with the best possible care. ◆

REFERENCES

1. Wood VE. The sesamoid bones of the hand and their pathology. *J Hand Surg* 1984; **9:** 261–4.
2. Major N, Malinzak MD. Netter's correlative imaging: musculoskeletal anatomy. 1st edn. Saunders, 2011.
3. Bianchi S, Martinoli C. Ultrasound of the musculoskeletal system. New York: Springer, 2007.
4. Van Onselen EB, Karim RB, Hage JJ, Ritt MJ. Prevalence and distribution of hand fractures. *J Hand Surg* 2003; **28:** 491–5.
5. Sletten IN, Nordsletten L, Hjorthaug GA, Hellund JC, Holme I, Kvernmo HD. Assessment of volar angulation and shortening in 5th metacarpal neck fractures: an inter- and intra-observer validity and reliability study. *J Hand Surg* 2013; **38:** 658–66.
6. Memarsadeghi M, Breitenseher MJ, Schaefer-prokop C, et al. Occult scaphoid fractures: comparison of multidetector CT and MR imaging–initial experience. *Radiology* 2006; **240:** 169–76.
7. Wheeldon FT. Recurrent dislocation of extensor tendons in the hand. *J Bone Joint Surg* 1954; **36:** 612–7.
8. Lopez-ben R, Lee DH, Nicolodi DJ. Boxer knuckle (injury of the extensor hood with extensor tendon subluxation): diagnosis with dynamic US–report of three cases. *Radiology* 2003; **228:** 642–6.
9. Klauser A, Frauscher F, Bodner G, et al. Finger pulley injuries in extreme rock climbers: depiction with dynamic US. *Radiology* 2002; **222:** 755–61.
10. Jacobson J. Fundamentals of musculoskeletal ultrasound. 2nd edn. Philadelphia: Elsevier, 2013; 142–3.
11. Ebrahim FS, De Maeseneer M, Jager T, et al. US diagnosis of UCL tears of the thumb and Stener lesions: technique, pattern-based approach, and differential diagnosis. *Radiographics* 2006; **26:** 1007–20.
12. Haugen I, Englund M, Aliabadi P, et al. Prevalence, incidence and progression of hand osteoarthritis in the general population: the Framingham Osteoarthritis Study. *Ann Rheum Dis* 2011; **70:** 10.1136.
13. Brant WE, Helms C. Fundamentals of diagnostic radiology. 4th edn. Philadelphia: Lippincott Williams and Wilkins, 2012.
14. Bassetti E, Candreva R, Santucci E. Giant cell tumor of the flexor tendon of the wrist: US and MRI evaluation. Case report. *J Ultrasound* 2011; **14:** 37–9.

Acknowledgements

Special thanks to the Radiology Department at The Robert Jones & Agnes Hunt Orthopaedic Hospital in Oswestry for permission to use Figures 11 and 12.